Super-resolution nanofabrication with metal-ion doped hybrid material through an optical dual-beam approach

Yaoyu Cao, Xiangping Li, and Min Gu

Citation: Applied Physics Letters **105**, 263102 (2014); doi: 10.1063/1.4905056
View online: http://dx.doi.org/10.1063/1.4905056
View Table of Contents: http://scitation.aip.org/content/aip/journal/apl/105/26?ver=pdfcov
Published by the AIP Publishing

Super-resolution nanofabrication with metal-ion doped hybrid material through an optical dual-beam approach

Yaoyu Cao, Xiangping Li, and Min Gu[a)]
Centre for Micro-Photonics, Faculty of Science, Engineering and Technology, Swinburne University of Technology, P.O. Box 218, Hawthorn, Victoria 3122, Australia

(Received 20 August 2014; accepted 15 December 2014; published online 29 December 2014)

We apply an optical dual-beam approach to a metal-ion doped hybrid material to achieve nanofeatures beyond the optical diffraction limit. By spatially inhibiting the photoreduction and the photopolymerization, we realize a nano-line, consisting of polymer matrix and *in-situ* generated gold nanoparticles, with a lateral size of sub 100 nm, corresponding to a factor of 7 improvement compared to the diffraction limit. With the existence of gold nanoparticles, a plasmon enhanced super-resolution fabrication mechanism in the hybrid material is observed, which benefits in a further reduction in size of the fabricated feature. The demonstrated nanofeature in hybrid materials paves the way for realizing functional nanostructures. © *2014 AIP Publishing LLC*.
[http://dx.doi.org/10.1063/1.4905056]

Direct laser writing with passive photopolymers has recently revolutionized the nano/micro-fabrication field and enabled a noninvasive and fast method for fabricating three-dimensional (3D) structures towards micro-devices with a resolution at the scale of the light wavelength.[1] By elaborately designing geometries of the structures, this technique has resulted in a growing number of applications, including optical data storage, micro-fluidic channels, bio-scaffolding, and optical waveguides. On the other hand, functionalities of the structures are much less exploited due to the passive photopolymer lack of native opto-electrical properties. In this regard, hybrid photopolymeric materials are developed for fabricating functional structures by incorporating optically active components like metal or semiconductor nanoparticles.[2–8] While the polymer matrix provides the backbones for self-supporting structures, the optically active nanocomponents can offer an exceptional platform for manipulating light mater interaction at the nanometer scale.

In addition to the functionalization of the structures, the physical barrier imposed by the diffraction nature of light sets up a limit to lateral resolution and hence the feature size of $\lambda/(2NA)$ (λ is the wavelength of the light and NA is the numerical aperture) in the fabrication of the structures. Even though some approaches including the polarization modulation,[6] multi-photon absorption,[9] chemical inhibition,[10] and high nonlinear photosensitivity[11] have been utilized to improve resolution, the focal spot with the size at the scale of the wavelength, as a result of the diffraction barrier of light, represents a fundamental obstacle to realize nanofeatures. On the other hand, the stimulated emission depletion (STED)-inspired direct laser writing has revealed that dual laser beams, enduing photo-initiated reactions with opposite functions such as photoinduction and photoinhibition, can break the diffraction barrier and achieve line structures with the feature size of sub 100 nm based on the passive photopolymeric materials by varying the intensity ratio of the two laser beams.[12–16] Combining with optically active components, theoretical studies even point out a way to further improve resolution and implement a low-power and low-cost scheme by employing metal nanoparticle induced local/near-field enhancement effect.[17] However, super-resolution nanofabrication of hybrid photopolymer composites with a sub 100 nm feature size has never been realized yet.

In this paper, we demonstrate a super-resolution fabrication technique for sub-100 nm resolution in gold-ion doped hybrid photoresin employing a dual-beam approach. Along with the polymer matrix formed by a photopolymerization process, gold particles can be *in-situ* produced through the photoreduction of doped gold ions. Two laser beams are used to conduct photoreactions during the fabrication, where one beam is responsible for inducing the reaction which can be inhibited by the other beam. By overlapping the two laser beams and tuning their power ratio, the line feature size of sub-100 nm is realized.

The experimental configuration of the optical dual-beam approach for super-resolution nanofabrication with the hybrid material is shown in Figure 1(a). One laser beam with a Gaussian shape, operating at the wavelength of 800 nm, works as the "induction beam" to excite the hybrid photoresin and generates active radicals. As shown in Figure 1(b), once the concentration of the active radicals is above the threshold, they can reduce the gold ions and trigger the formation of gold particles at the center of the laser focal spot.[18] Meanwhile, the generated gold nanoparticles can be solidified in the polymer matrix through the accompanied polymerization process. The other laser beam at the wavelength of 532 nm working as the inhibition beam is modulated to the Laguerre-Gaussian mode to inhibit the polymerization and photoreduction at the peripheral region of such formed doughnut-shaped focal spot. Despite lacking of the ability to excite the hybrid photoresin, the inhibition beam can prohibit the generation of radicals by deactivating radical-generation precursor in the hybrid photoresin.[19] With the overlapping of the two laser beams, the radical generation can be inhibited in the ring of the inhibition beam and

[a)]Email: mgu@swin.edu.au

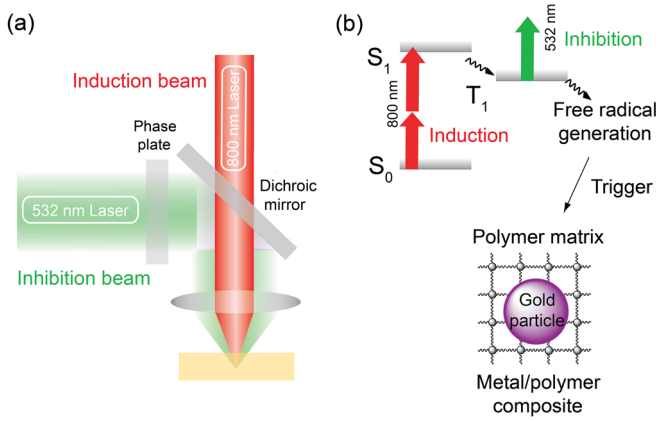

FIG. 1. Schematic of the super-resolution fabrication in a metal-polymer hybrid material by the optical dual-beam approach. (a) The optical fabrication system. The laser beam at the wavelength of 532 nm working as the inhibition beam is modulated to a doughnut mode by a vortex phase plate (0 to 2π). The inhibition beam combined with a Gaussian shaped induction beam at the wavelength of 800 nm is focused into the hybrid photoresin through a single objective. (b) The optical induction/inhibition process conducted by two laser beams. The femtosecond (fs) induction beam can induce the formation of solidified metal/polymer composite through multiphoton absorption process of the dye isopropylthioxanthone. The CW inhibition beam can inhibit the generation of active radicals[19] and prevent the following photoreduction and photopolymerization reactions. S_0, S_1, and T_1 represent the dye isopropylthioxanthone of the ground state, the first singlet state, and the first triplet state, respectively.

localized in the center of the focal spot of the induction beam. The variation of the power ratio of the two beams allows for tuning the photoreduction area as well as the zone where the polymer matrix is formed.

The choice of the hybrid photoresin is critical to realize the super-resolution fabrication of nanofeatures. The photoresin should be capable of dissolving the metal ions to form a transparent solution without significant thermal reduction of the metal ions and contain photosensitive radical-generation precursors that can be photo-deactivated at their excited state. To this purpose, the hybrid photoresin is prepared by mixing a monomer of SR 444 (Sartomer), a radical-generation precursor of isopropylthioxanthone with a content of 3 wt. %, and a salt of tetrachloroauric acid (HAuCl4) with a content of 0.5 wt. %. The tetrachloroauric acid and the isopropylthioxanthone are first dissolved in chloroform separately and then mixed with SR 444. The mixture is kept in the oven at the temperature of 50 °C for 12 h to remove chloroform and concentrate the photoresin. For exciting the hybrid photoresin and triggering the photoreduction, a femtosecond laser beam at the wavelength of 800 nm (a pulse width of 140 fs and a repetition rate of 80 MHz) is employed. A continuous wave (CW) laser beam at the wavelength of 532 nm is used as the inhibition beam. The two laser beams are combined by a dichroic mirror and focused by an objective with the NA of 1.4. To prepare the sample for the fabrication, the hybrid photoresin is sandwiched by two coverslips with a spacer layer of ~40 μm. Arbitrarily designed structures can be fabricated by scanning the overlapped focal spots of the dual beams across the sample mounted on a computer controlled piezo stage. After the fabrication, the sample is washed with isopropanol for 5 min. The final feature sizes of the lines as fabricated are measured by a Zeiss Supra 40 VP Field Emission Scanning Electron Microscope (SEM) with an imaging resolution of 2 nm.

The single-photon absorption spectra for a thin film of the hybrid material, as shown in Fig. 2(a), are measured before and after the exposure to a ultra-violet (UV) lamp for 5 min. An absorption band from 520 nm to 560 nm that is the typical plasmonic resonance band of gold nanoparticles shows up after the exposure to the UV light, while the hybrid photoresin is solidified through polymerization. The absorption band for the hybrid photoresin (reference sample) is up to 450 nm, which implies that the photo-induced chemical reactions are attributed to a multiphoton absorption process by the exposure to the induction beam at the wavelength of 800 nm. The inhibition beam at the wavelength of 532 nm fallen in the emission tail of the dye isopropylthioxanthone is employed for the photodeactivation, as shown in Fig. 2(b), which prevents the excitation of the photoresin by the inhibition beam and the resultant unwanted physical and chemical changes.

As the photoreduction of metal ions is based on the electron transfer, the formation speed of gold nanoparticles can be much faster than the formation of polymer matrix during the fabrication process. In this regard, the fabrication threshold is largely governed by the polymerization process. For the sample containing HAuCl4 with a content of 0.5 wt. %, the minimum laser power of the line fabrication is 8 mW, at a scanning speed of 125 μm/s, measured at the back aperture

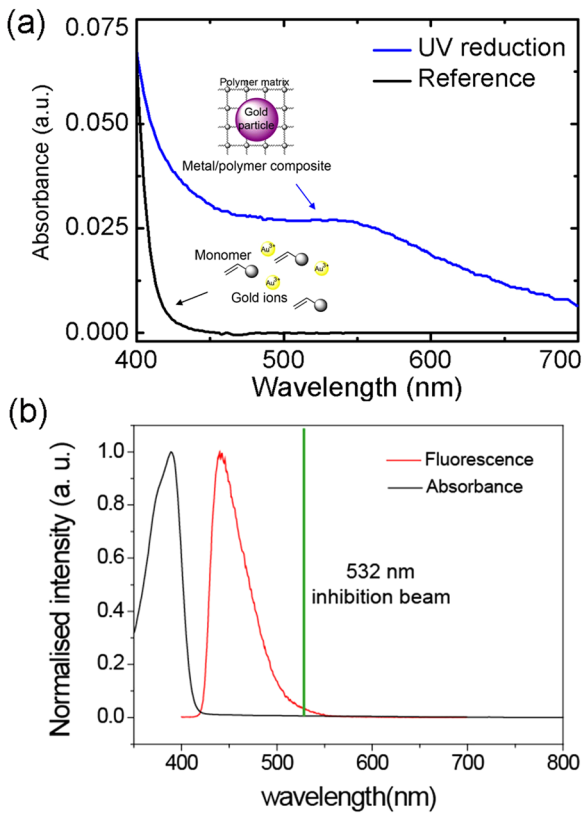

FIG. 2. (a) The single-photon absorption spectra of the hybrid photoresin before (reference) and after the exposure to UV light. (b) The single-photon absorption and fluorescence spectra of the radical generator isopropylthioxanthone in chloroform. The fluorescence spectrum reflects the excited state electron configuration of isopropylthioxanthone. The wavelength of the inhibition beam can be selected at the red tail of the emission band to avoid the re-excitation of the radical generator and ensure the inhibition process.[14]

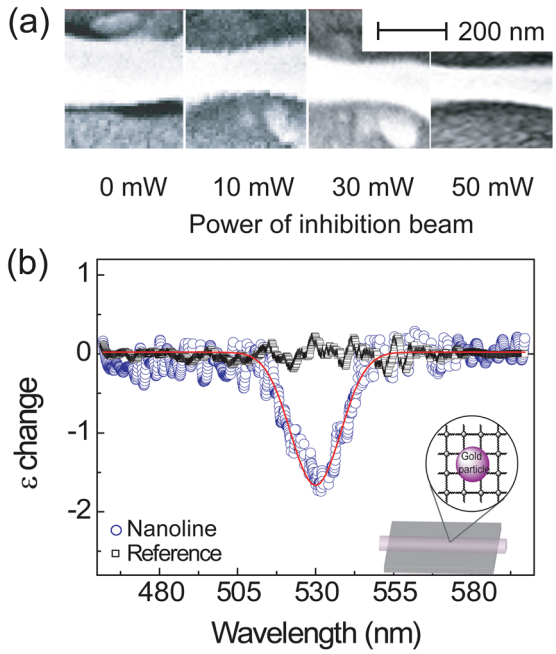

FIG. 3. (a) SEM images of lines fabricated with varied powers of the inhibition beam. (b) The transmission spectra of the hybrid photoresin prior to the fabrication (reference) and the sub 100 nm nano-line fabricated by the dual-beam approach. The negative change of the extinction coefficient (ε change) represents the decrease of the light transmittance due to the absorption and scattering by gold nanoparticles in the nano-lines.

of the objective, which is equal to that used for the sample prepared without HAuCl4 salt. The SEM images of typical lines fabricated by dual laser beams at different powers of the inhibition beam are shown in Fig. 3(a). In case of the fabrication without the inhibition beam, the multiphoton absorption induced chemical reaction gives the linewidth of 200 nm. By increasing the power of the inhibition beam, the linewidth decreases to deep sub-wavelength scale beyond the diffraction limit. This can be attributed to the inhibition beam induced photodeactivation of the isopropylthioxanthone which prevents the formation of free radicals to trigger the photoreduction and the photopolymerization.[19] At the inhibition power of 50 mW, the linewidth of sub 100 nm is realized, which corresponds to around 50% improvement compared to the diffraction limited multiphoton fabrication.

To confirm the generation of gold nanoparticles in the nano-lines, we used a confocal microscope system to obtain the transmission spectra of the nano-lines with a lamp as the light source. In the measurement, while an objective with the NA of 0.4 was used to focus the white light on to the lines, the transmitted light was collected by another objective on the opposite side with the same NA. The transmission spectra for the sub 100 nm nano-line, shown in Fig. 3(b), reveal the extinction peak located at around 530 nm, which agrees with the absorption peak measured in bulk materials exposed to the UV irradiation. The extinction peak can be attributed to the localized surface plasmonic resonance of the gold nanoparticles formed in the lines. Thus, both of the photoreduction and the polymerization with the hybrid photoresin are clearly confined in the sub-100 nm scale, corresponding to around 1/7 of the diffraction limited focal spot of the induction beam. (The induction beam can be focused into a 690 nm spot based on Abbe's law, given the experimental condition with the induction beam wavelength of 800 nm and the NA of 1.4.)

By comparing the super-resolution fabrication of hybrid material with the sample without doped gold ions, we found that the photoactive gold components play a role in determining resolution for a given fabrication condition, shown in Table I. Whilst the increase of the inhibition beam power leads to decreased linewidth for samples either with or without doped gold ions, the absolute value of the decrease for the sample with gold ions outweighs its counterpart, which suggests greater inhibition efficiency. As the wavelength of the inhibition beam is located in the plasmonic resonant frequency range of gold nanoparticles (Fig. 2), the increased inhibition efficiency might be attributed to the field enhancement attained by the excitation of the nanoparticle plasmonic resonance.[17]

Since the feature size of the lines as fabricated is governed by the inhibition efficiency $\eta_{inh}(r)$ that can be expressed as the probability of the free radical generation decay, r, denoting the distance from a point to the center of the induction beam, we studied the variation of the feature size against the intensity of the inhibition beam. With a CW inhibition beam, the probability of the free radical generation decay $\eta_{inh}(r)$ can be approximately given as[20]

TABLE I. Experimentally measured and fitting values of line feature size versus the power of the inhibition beam. The induction beam is at a constant power of 8 mW and the scanning speed is 125 μm/s.

	Without gold ions	With 0.5% $HAuCl_4$		
Power of inhibition beam (mW)[a]	Feature size (D_1) (experimental) (nm)[b]	Feature size (D_2) (experimental) (nm)[b]	Feature size (D_2') (fitting) (nm)[c]	Feature size reduction (%)[d]
0	202	201	204	0.5
10	180	170	168	5.6
30	152	127	121	16.4
50	107	98	100	8.4
60	101	108	104	−6.9

[a]Power levels of the inhibition beam of 0, 10, 30, 50, and 60 mW correspond to the intensity ratio of the inhibition beam to the induction beam of 0, 1.25, 3.75, 6.25, and 7.5, respectively.
[b]The feature size, which is measured by the full width at half maximum of each line, is averaged by more than ten lines for each power of the inhibition beam.
[c]The feature size is determined by the probability to generate free radicals, $h(r)_{plus}$. The α, β, and I_s values are 1.09, 2.64, and 42.5 MW/cm^2, respectively, found in the fitting based on Eqs. (3)–(5).
[d]The feature size reduction % is calculated by $(D_1 - D_2)/D_1$.

$$\eta_{inh} \approx (1 + \alpha I_{inh}/I_s)^{-1}, \quad (1)$$

where $I_{inh}(r)$ represents the intensity of the inhibition beam at a point of r, α is a constant encompassing the plasmonic effect caused by the gold particles, and I_s denotes the saturated intensity. Thus, the probability to generate free radicals $h(r)$ at r can be expressed as

$$h(r) = \Phi_{rad} h_{exc}(r) \eta_{inh}(r), \quad (2)$$

where Φ_{rad} (0.003) represents the probability to form free radicals upon the excitation by the induction beam and $h_{exc}(r)$ is the excitation probability. For a focused induction beam, we have

$$h_{exc} = A \cos^2(\pi r NA/\lambda_{ind}), \quad (3)$$

$$\text{and} \quad I_{inh} = I_0 \sin^2(\pi r NA/\lambda_{inh}), \quad (4)$$

λ_{ind} and λ_{inh} denoting the wavelength of the induction beam and the inhibition beam, respectively. In addition, it should be noted that an increase factor of the free radical generation probability as a result of the photoabsorption by gold particles cannot be neglected in case of using high power of the inhibition beam.[21,22] Thus, $h(r)$ needs to be modified to take the photoabsorption effect into consideration

$$h(r)_{plus} = \Phi_{rad} h_{exc}(r)[\eta_{inh}(r) + \eta_{abs}(r)], \quad (5)$$

where $\eta_{abs}(r) = \beta(1 + I_c/I_{inh})^{-1}$ is the increase of the free radical generation probability caused by the photoabsorption of gold nanoparticles, β is a constant encompassing the content and the size of the gold nanoparticle. In this case, the feature size of nano-lines obtained from the fitting qualitatively agrees with the experimental results, as shown in Table I. When the inhibition beam power of 30 mW is used, it reveals that the sample doped with gold ion results in the feature size of 16.4% less than its counterpart, illustrating that the plasmonic enhancement effect benefits in producing smaller features at a relatively low inhibition power. Further increasing the inhibition beam power, a turning point of the feature size is observed. Enlarged feature size appears once the inhibition beam power exceeds 60 mW, as a result of the photoabsorption effect of gold nanoparticles.

In conclusion, we have realized an optical dual-beam super-resolution fabrication technique at the scale far beyond the diffraction limit in a metal-ion doped hybrid photoresin. By optimizing the power ratio between the induction beam and the inhibition beam, we achieved sub-100 nm polymer lines embedded with gold nanoparticles. In addition, plasmon enhanced super-resolution fabrication has been observed. The demonstrated optical dual-beam fabrication technique based on metal-ion doped hybrid material paves the way to prepare metal doped nanostructures with super-resolved feature size for plasmonic and metamaterial applications.[23] It is also promising for super-resolution nanofabrication of hybrid material with flexible active components in developing micro-/nano-devices towards a broader range of applications in the field of photovoltaic, biosensing, 3D display, and so on.

This work was supported by the Australian Research Council (ARC) the Laureate Fellowship scheme (FL100100099).

[1]S. Kawata, H. Sun, T. Tanaka, and K. Takada, Nature **412**, 697 (2001).
[2]S. Shukla, X. Vidal, E. P. Furlani, M. T. Swihart, K.-T. Kim, Y.-K. Yoon, A. Urbas, and P. N. Prasad, ACS Nano **5**, 1947 (2011).
[3]K. Vora, S. Kang, S. Shukla, and E. Mazur, Appl. Phys. Lett. **100**, 063120 (2012).
[4]X. Li, T. H. Lan, C. H. Tien, and M. Gu, Nat. Commun. **3**, 998 (2012).
[5]H. Xia, J. Wang, Y. Tian, Q. Chen, X. Du, Y. Zhang, Y. He, and H. Sun, Adv. Mater. **22**, 3204 (2010).
[6]X. Li, Y. Y. Cao, and M. Gu, Opt. Lett. **36**, 2510 (2011).
[7]X. Li, J. W. M. Chon, R. A. Evans, and M. Gu, Opt. Express **17**, 2954–2961 (2009).
[8]X. Li, Q. Zhang, X. Chen, and M. Gu, Sci. Rep. **3**, 2819 (2013).
[9]T. Tanaka, A. Ishikawa, and S. Kawata, Appl. Phys. Lett. **88**, 081107 (2006).
[10]Y.-Y. Cao, N. Takeyasu, T. Tanaka, X.-M. Duan, and S. Kawata, Small **5**, 1144 (2009).
[11]Y. Y. Cao and M. Gu, Appl. Phys. Lett. **103**, 213104 (2013).
[12]L. Li, R. R. Gattass, E. Gershgoren, H. Hwang, and J. T. Fourkas, Science **324**, 910 (2009).
[13]T. F. Scott, B. A. Kowalski, A. C. Sullivan, C. N. Bowman, and R. R. McLeod, Science **324**, 913 (2009).
[14]J. Fischer and M. Wegener, Opt. Mater. Express **1**, 614 (2011).
[15]Y. Y. Cao, Z. S. Gan, B. H. Jia, R. A. Evans, and M. Gu, Opt. Express **19**, 19486 (2011).
[16]Z. S. Gan, Y. Y. Cao, R. A. Evans, and M. Gu, Nat. Commun. **4**, 2061 (2013).
[17]Y. Sivan, Y. Sonnefraud, S. Kéna-Cohen, J. B. Pendry, and S. A. Maier, ACS Nano **6**, 5291 (2012).
[18]Y. Yonezawa, T. Sato, S. Kuroda, and K. Kuge, J. Chem. Soc., Faraday Trans. **87**, 1905 (1991).
[19]B. Harke, W. Dallari, G. Grancini, D. Fazzi, F. Brandi, A. Petrozza, and A. Diaspro, Adv. Mater. **25**, 904 (2013).
[20]M. Leutenegger, C. Eggeling, and S. W. Hell, Opt. Express **18**, 26417 (2010).
[21]S. Nah, L. Li, R. Liu, J. Hao, S. B. Lee, and J. T. Fourkas, J. Phys. Chem. C **114**, 7774 (2010).
[22]M. Maillard, P. Huang, and L. Brus, Nano Lett. **3**, 1611 (2003).
[23]M. Gu, X. Li, and Y. Y. Cao, Light: Sci. Appl. **3**, e177 (2014).